Earth and Planetary Science Letters, 95 (1989) 341–358
Elsevier Science Publishers B.V., Amsterdam – Printed in The Netherlands

[5]

Modeling crustal phases in southeast France for focal depth determination

Didier Bertil [1], Nicole Bethoux [2], Michel Campillo [3] and Bernard Massinon [1]

[1] *Laboratoire de Géophysique, L.D.G. du C.E.A., B.P. 12, 91680 Bruyères le Chatel (France).*
[2] *Centre Scientifique de Monaco, 16 bd de Suisse, Monaco (Monaco)*
[3] *Observatoire de Grenoble, Université Joseph Fourier (U.R.A. CNRS 733), IRIGM, B.P. 53X, 38041 Grenoble Cedex (France)*

Received January 26, 1989; revised version accepted July 8, 1989

In numerous regions, the focal depths are not precisely determined from standard location methods because of the poor azimuthal coverage by the seismic network or because of the important geological complexity. In this study, we attempt to refine the determination of the focal depth of some events by analyzing the waveforms of the seismograms and the relative amplitude of the crustal phases. The discrete wave number representation method is used to compute synthetics corresponding to sources at various depths. We present three examples of events which occurred in southeast France in different geological units. We conclude that the waveforms are not very sensitive to slight changes of the crustal model or quality factors, but are very dependent on the focal depth. If a convenient crustal model is used in the computations, the numerical simulations constrain the depth in a better way than standard location methods using arrival times. In our examples, when the path from source to station crosses different structures, the best fit of the envelope of the seismograms by synthetics computed in a flat-layered model is reached for a crustal model corresponding to the source region.

1. Introduction

In most seismic areas, the analysis of arrival time from seismological networks does not allow constraint of the depth of hypocenters because of poor azimuthal coverage of the stations and also because of regional geological complexity which implies strong variations of the propagation laws.

In southeast France the crustal structures and the regional tectonics are relatively well known. This zone is a complex area which includes the Ligurian Sea, characterized by its oceanic crust [1,2], the heterogeneous region of the southwestern Alps and the crystallophyllian massifs of Maures and Esterel (Fig. 1). This complexity results in a great difficulty to obtain accurate hypocentral locations. Also resulting from this complexity is the different apparent attenuation observed, according to the region crossed by the ray-paths.

The simulation of wave propagation at regional distance, in simple flat-layered media, provides synthetic seismograms in remarkable agreement with the observations, at least in stable continental areas. Such results have been shown both in the time domain [3–5] and in the frequency domain [6]. Among other techniques, the discrete wave number representation method [7,8] allows one to compute the exact response of a stack of viscoelastic layers to any type of dislocation source. In this study, we attempt to improve the precision of the focal depth and of the quality factors by analyzing the waveforms of crustal phases. These parameters will be tested by iterative modeling in a trial-and-error process.

According to theoretical investigations [9], the amplitude ratios between the wave trains (P, S, P_n, P_g and L_g) exhibit strong variations when the source depth is changed. The multireflected L_g phase is particularly sensitive to focal depth. This phase becomes important at distances larger than the critical distance of Moho reflection. In order to get prominent L_g and relatively simple waveforms, we only consider in this work, seismograms in the distance range from 80 to 160 km. We study here three earthquakes recorded by the stations of the L.D.G. network (Fig. 1) located within this epicentral distance range. The first event (M_l = 3.3) occurred in the southern Alps, the second

0012-821X/89/$03.50

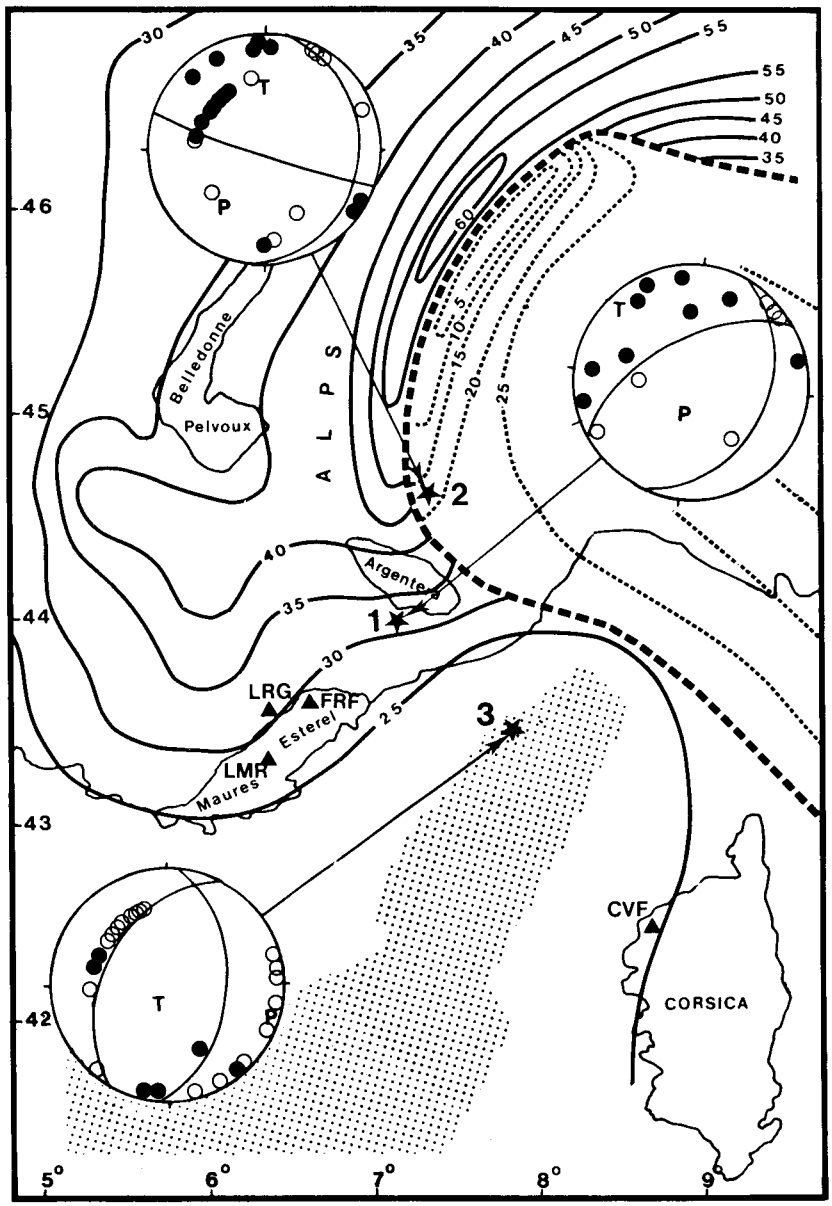

Fig. 1. Location of epicenters and recording stations. The stars indicated by numbers *1*, *2*, *3* represent epicenters of the events on September 2, 1982 ($M_l = 3.3$), on January 12, 1984 ($M_l = 3.6$), and on October 4, 1985 ($M_l = 3.9$). The focal mechanisms computed for these events are superimposed. The seismic stations used are denoted by triangles. The Moho depth beneath France is reported in heavy lines, according to compilations by Hirn [23] and Meissner [24]. The Moho depth beneath Apulo-Adriatic plate is indicated by the dashed lines, after Morelli et al. [25]. The stippled area of the Ligurian Sea is interpreted as oceanic basement and/or stretched continental crust after Rehault et al. [26].

($M_l = 3.6$) in the Ivrea zone and the third ($M_l = 3.9$) beneath the Ligurian Sea. Their focal mechanisms are displayed in Table 1 and Fig. 1.

The influence of the mechanism on the waveform will be discussed shortly. A preliminary study allowed us to evaluate average values for the quality factors Q_s from spectral analysis of L_g waves beneath the seismic network. For this area the average quality factor Q_s was found to be of the form: $200f^{0.60}$, where f is the frequency. In the

absence of firm information about Q_p we assume a theoretical ratio $Q_p/Q_s = 2$, following the definition of the internal friction $Q - 1$ [11].

The source time function used for the synthetics is a smooth ramp with a rise time of 0.2 s. The theoretical ground displacements were convolved with the short period seismograph response (vertical component) of the L.D.G. stations [12]. In order to compare the synthetics with observed seismograms, all the signals were filtered between 0.5 and 5 Hz.

2. Earthquake of Roquebillere, southern Alps

The first event we consider occurred on September 2, 1982. The hypocenter computed by E.M.S.C. is: 44° N ± 0.02°, 7.10° E ± 0.03°, Z = 10 km, close to the small city of Roquebillere, whereas the location from the L.D.G. network is given with an undetermined focal depth (see point *1*, Fig. 1). In order to determine the depth of this event, we compute the seismogram recorded at the station LMR at an epicentral distance of 93 km (Fig. 1). For this station the ray-path is very close to a profile of deep seismic sounding: the line "lac Nègre–Provence", studied by Recq [13]. The crustal model used is deduced from the interpretation proposed by this author (Table 2). The focal mechanism that we computed corresponds to a normal fault motion (Table 1).

2.1. *Effect of source depth*

Synthetics obtained with different source depths (28, 20, 15, 10, 4 and 1.5 km) are presented in Fig. 2. The waveform and relative amplitude of the synthetics are strongly sensitive to the focal depth. For each computation, the maximum of L_g wave amplitude (velocity component), is reported in hundredths of millimeter per second for a seismic moment of 10^{23} dynes cm. This maximum decreases strongly when the focal depth increases. When the source is located in the sediments the energy is mainly trapped in the shallow layers in the form of Rayleigh waves which have very large amplitude and low group velocities. They give rise to very particular waveforms in the seismograms. We may observe a clear decrease of the coda duration as the source depth increases. Except when the source is in the mantle or in the sediments, the P_g waves amplitude stays almost unchanged whatever the depth of the focus. This results in a larger P_g/L_g amplitude ratio for deeper intracrustal sources, as previously noticed by Campillo et al. [9]. Except for the deepest sources (20–30 km), the first arrival times are very similar (which explains the inaccuracy of depth determination by usual location techniques), while P_g waves exhibit very different aspects according to the layer where the source is. So, with respect to the envelope of the S-wave train and the energy distribution in the P-wave train the best agreement between observed and synthetic seismograms is obtained for a depth of 4 km.

We investigated in detail the effect of source depth around 4 km. Considering a source located respectively at 4.5, 4 and 3.5 km, the arrival times of the different energy pulses and the shape of the coda lead us to conclude that it is for the depth of 3.5 km that the synthetic seismogram fits the actual one the most accurately (Fig. 3).

2.2. *Discussion*

We will investigate the effect of quality factors on the synthetics. In the previous computations

TABLE 1

Fault-plane solutions for the three events studied. Solutions used in this study and which are in good agreement with the tectonics [10] are given first. These focal mechanisms are reported in Fig. 1. Other solutions close to the previous ones and also relatively coherent with the distribution of the first motions are shown in parentheses. They were also tested by modelization

Date	Time (h:min:s)	M_l	Location	Depth (km)	Plane A	Plane B	P	T
2 Sep 82	21:45:25	3.3	44.00° N, 7.20° E	10	55 W 60	20 E 35	185–69	311–13
					(38 W 56	55 E 35	97–77	315–11)
12 Jan 84	8:24:46	3.6	44.66° N, 7.35° E	– *	05 E 20	108 W 85	215–37	358–46
					(350 E 65	96 W 59	44–04	171–41)
4 Oct 85	15:22:11	3.9	43.64° N, 8.09° E	12	30 W 45	05 E 48	107–01	204–77
					(350 W 61	61 E 60	115–01	26–45)

* Not determined.

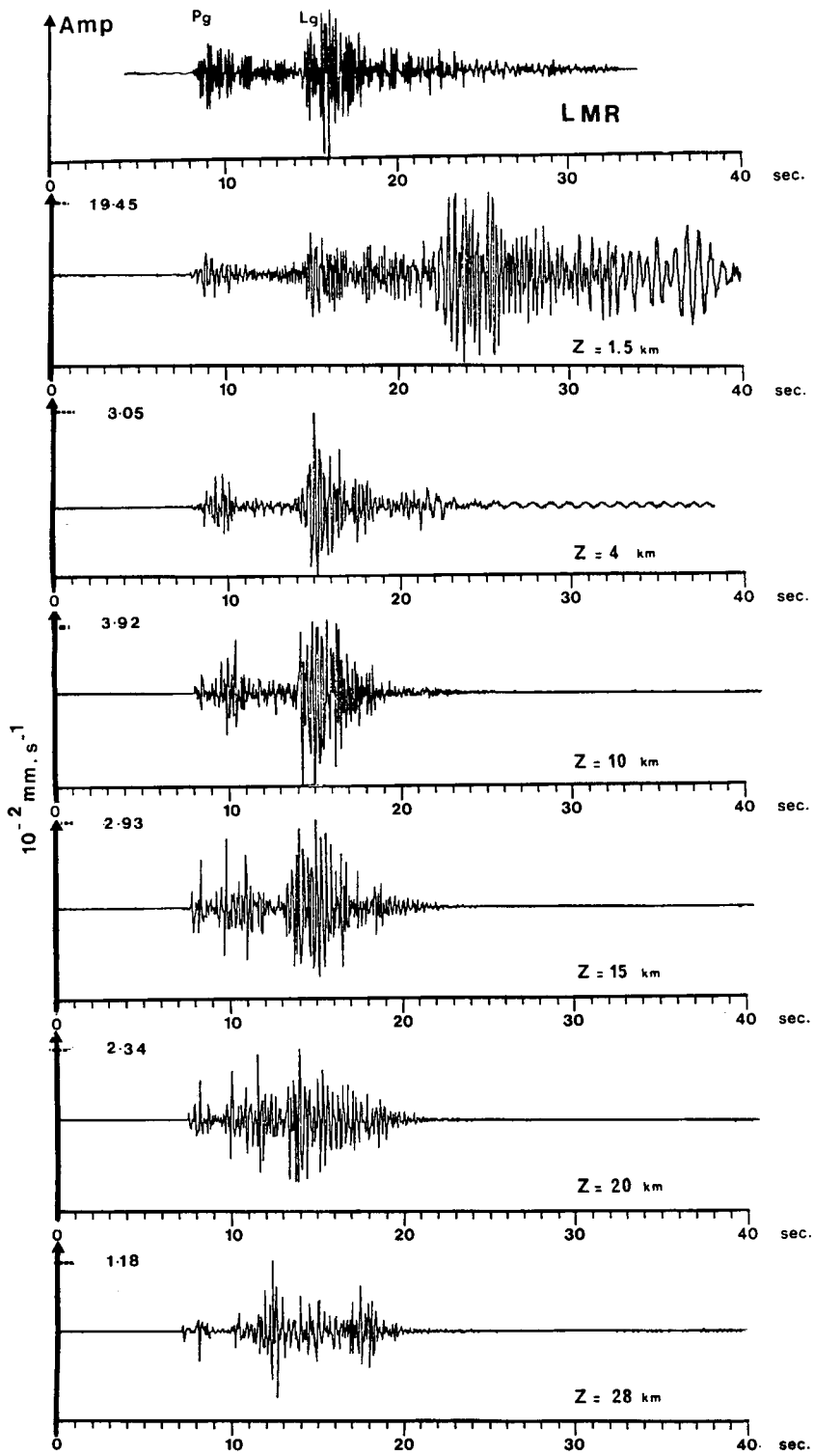

Fig. 2. Synthetic seismograms (z velocity component) computed at various depths corresponding to an epicentral distance of 3.5 km for event 1 by using the crustal model of Table 2. Each signal is normalized and the amplitude of the maximum is given in hundredths of a millimeter. These seismograms are compared with the observed record at station LMR.

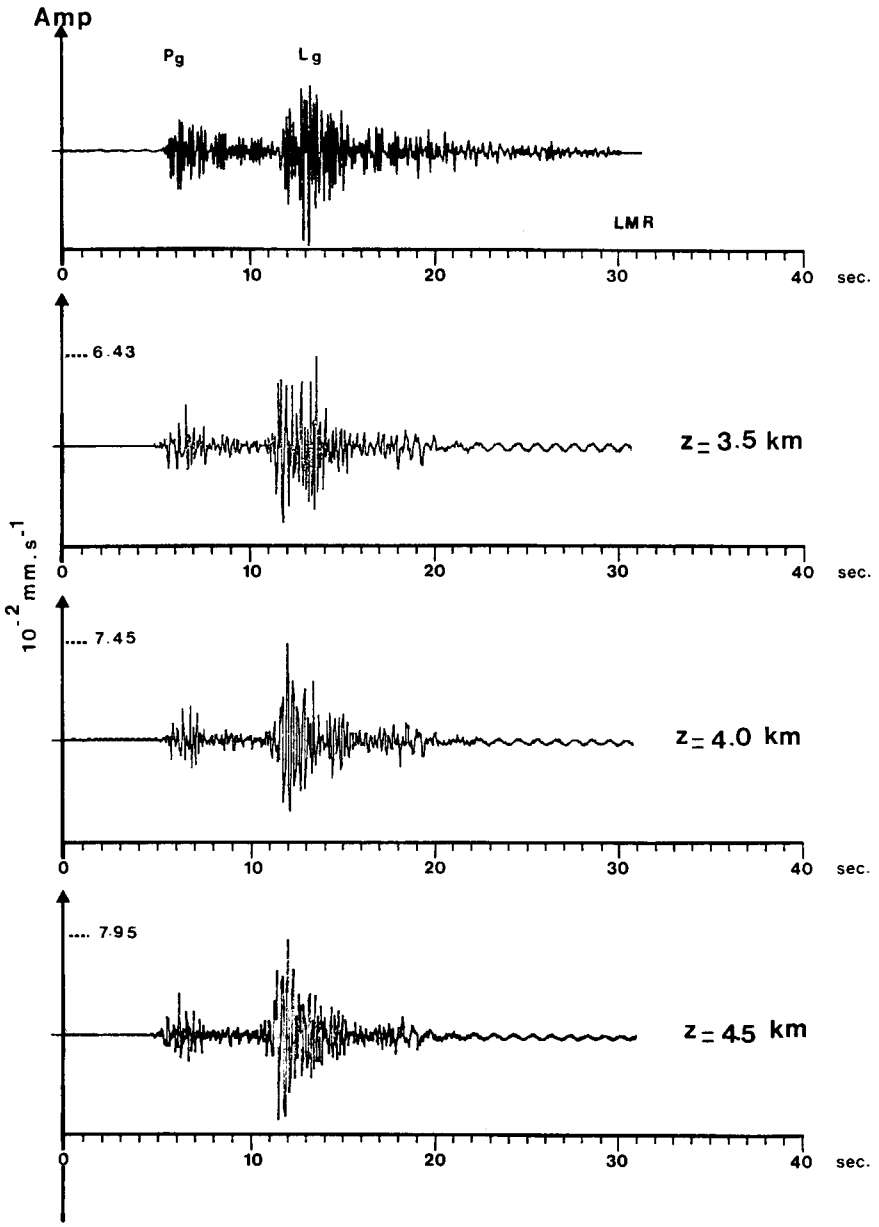

Fig. 3. Seismograms corresponding to the fitting of the source depth for event 1. The epicentral distance and crustal parameters are the same as in Fig. 2.

we have considered Q_p and Q_s to be independent of depth. Now, we choose quality factors increasing with depth as suggested by different studies [6,14–18].

First, we consider a model with a lower attenuation in the thick bottom layer while Q values in the upper crust remain unchanged (Table 2b). The synthetic seismogram computed is depicted in Fig. 4B. The comparison with the results obtained with the initial model (Fig. 4A) indicates that this gradient of attenuation leads to a better distribution of energy among S waves and a more realistic synthetic.

Next, we investigate the effect of an increase of the quality factor in the upper crust. The model is presented in Table 2(c) and leads to the synthetic

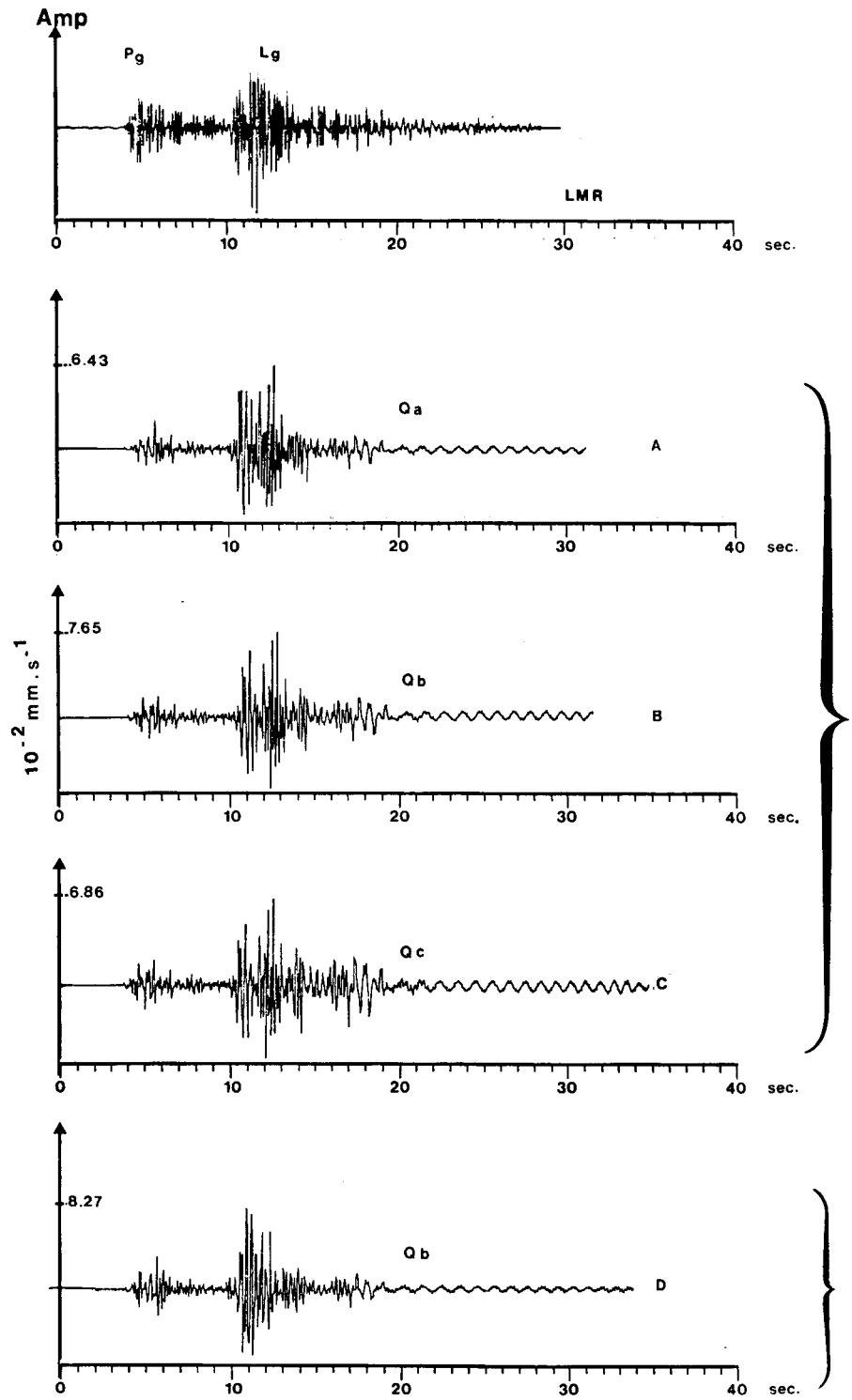

Fig. 4. Modelizations obtained with different quality factors. The synthetic traces A, B and C are computed by using a focal depth of 3.5 km and quality factors given in Table 2(a, b, c, respectively). D corresponds to computed wave-trains obtained for a depth of 4.5 km and quality factors shown in Table 2(c).

TABLE 2

Crustal model and different Q_s quality factors used for event 1, with $Q_p = 2Q_s$

Layer thickness km	P-wave velocity (km/s)	S-wave velocity (km/s)	Density (g/cm^3)	(a) Q_s	(b) Q_s	(c) Q_s
1	3.00	1.73	2.00	200	50	100
1	4.50	2.60	2.60	200	100	200
4	5.80	3.40	2.80	200	200	350
20	6.20	3.65	2.90	200	400	400
	8.05	4.70	3.30	99999	99999	99999

depicted in Fig. 4C. That shows the relatively weak sensitivity of the signal to a change of quality factor limited to the first kilometers of the crust. The comparison with the result obtained with the same crustal model but with a slightly different source depth (4.5 km in place of 3.5 km) shown in Fig. 4D, indicates the prominent part played by the focal depth on the waveform, in spite of the fact that the source remains in the same layer. This is a fundamental point that we will investigate shortly in the present example.

The possibility of focal depth determination is, of course, dependent on the knowledge of a realistic crustal structure. In order to evaluate the sensitivity of the seismograms to the characteristics of the model, we studied the effects of perturbations of the velocity distribution. The crustal models including small changes with respect to the reference model previously used, are presented in Fig. 5 (right) with the corresponding synthetics. The observed seismogram and the synthetic computed with the starting crustal model, depicted on the right of the figure, are reported in Fig. 5A.

—The lack of the first sedimentary layer drastically diminishes the complexity of P and S waves (Fig. 5B).

—In contrast a 1 km thicker sedimentary layer introduced in the computation leads to a synthetic with a more important coda (Fig. 5C). Nevertheless, the shape of the seismogram is not strongly disturbed in comparison with the initial synthetic of Fig. 5A.

—If we consider now a 2 km thicker upper crust the change of the computed synthetic is very small and only involves a different ratio in the energy pulses of S waves (Fig. 5D).

—A 2 km deeper Moho weakens the last part of L_g and the reflected P waves (Fig. 5E).

—Finally a smoother velocity increase is postulated in the lower crust. The synthetics obtained by assuming again a source depth of 3.5 km has a slightly stronger amplitude (Fig. 5F). This synthetic remains in good agreement with the observed seismogram.

From this example we conclude that focal depth determination is not critically dependent on the details of the crustal model considered. On the other hand, if the crustal model used is too different, we cannot obtain a realistic synthetic even by changing the focal depth. For example, the lack of a sedimentary layer produces a clearly simpler seismogram whatever the depth is. In a case of a slightly deeper Moho, the effect is much less dramatic. Especially, the L_g wave train is modified because a stronger geometric attenuation weakens these multireflected waves. Although weaker, this effect exists for the reflected P waves. Thus, we tried to compute a seismogram with a new depth (5.5 km) which kept the vertical distance from the focus to the Moho. The corresponding synthetic is not so realistic as the previous one, because of the modification of the incidence angle of the waves in the upper crust.

We may conclude that the focal depth determination seems reliable in this example. In many cases, this type of study allows us to obtain accurate evaluation of the focal depth while standard methods using arrival times give only precise determination of the epicenter. The main limitation seems to be that the crustal structure along the path should be uniform and of course known. In the next example we consider a case where the

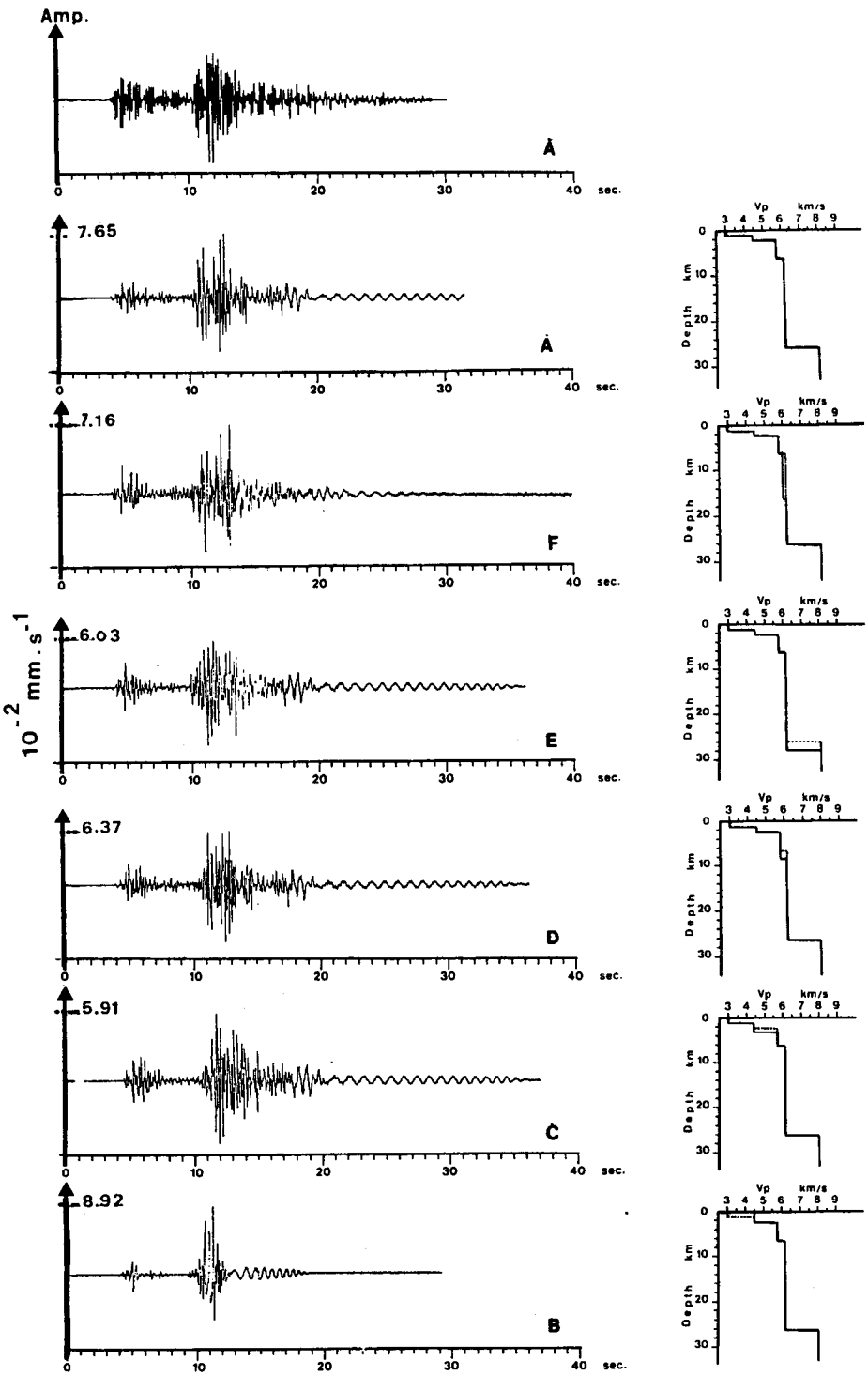

Fig. 5. Synthetics obtained for slight changes of the crustal model depicted on the right of the figure. The change of a layer is superimposed on the starting crustal model. Quality factors and source depth are the same as for Fig. 4.

structure is changing drastically from the source area to the receiver.

3. An earthquake in the Ivrea body

This event occurred on January 12, 1984, located at 44.7° N ± 0.02°, 7.3° E ± 0.03°, in the Ivrea zone, with an undetermined depth, according to the L.D.G. and the "Istituto Geofisico di Genova". We model the seismograms recorded in stations FRF, LRG, LMR, respectively 134, 156, 162 km away from the epicenter. The focal mechanism is a strike-slip fault (Table 1). The anomalous character of the Ivrea zone is well known [15,19,20]. So, a high-velocity layer is added in the crustal model in order to simulate the slice of the overthrusting upper mantle. The quality factors used are the same as in the first simulation (Table 3,a).

3.1. Effect of focal depth

The lack of strong Rayleigh waves on the observed seismograms (see Fig. 6A for station LMR) excludes the hypothesis of a very shallow focus. Thus, the depths 29, 21, 10 and 5 km were investigated at first (Fig. 6). Considering station LMR, the synthetic waveforms obtained for a 10 km deep source are the most similar to the records.

By performing further computations, we checked the effect of focal depth from 8 to 12 km. With respect to the envelope of the S wave-train and the distribution of the energy pulses in P and S waves, a intermediate value between 8 and 10 km is proposed. The corresponding synthetics for stations LRG and FRF are presented in Fig. 7B–D.

3.2. Discussion

We may verify the effect of a different gradient of attenuation in the crustal layers. The synthetic seismograms displayed in Fig. 7 are computed with quality factors given in Table 3(b) and with $Q_p = 2Q_s$. These new values allow us to model rather well the relative amplitude of the different energy pulses observed in the wave trains. In order to enhance this improvement, a ratio $Q_p = Q_s$ is now used (Table 3,c). The synthetics displayed in Fig. 8B, corresponding to a focal depth of 10 km and stations FRF and LRG are computed with these new Q_p values. The comparison with the Fig. 7B, where the signals are calculated with $Q_p = 2Q_s$ shows that the energy pulses of P waves fit now the observed ones more accurately. Indeed, in this case, a realistic P/S amplitude ratio needs weak Q_p values. This strong apparent attenuation should be due to the lateral heterogeneities of the medium.

As it was previously pointed out in this example, the structure encountered along the path between the source and the receivers presents strong lateral changes. We have to test the implications on the seismigrams of the choice of the crustal model, introduced in the computations, which we assumed to be plane and homogeneous.

Fig. 8B show the results obtained for stations LRG and FRF with the crustal model displayed in Table 3 taking into account the Ivrea Body.

If the anomalous character of the source region is ignored and the synthetics computed with the same crustal model used for the earthquake in Roquebillere (Table 2), the theoretical P/S amplitude ratio is too high with respect to the observed one (Fig. 8C). The S wave form is also modified.

If we consider a model in which the Moho is 40

TABLE 3

Crustal model and different quality factors used for event 2. In the cases (a) and (b) $Q_p = 2Q_s$

Layer thickness (km)	P-wave velocity (km/s)	S-wave velocity (km/s)	Density (g/cm^3)	(a) Q_s	(b) Q_s	(c) Q_p	(d) Q_s
1	3.50	1.70	2.00	100	50	50	50
1	4.50	2.60	2.60	200	100	100	100
4	5.80	3.40	2.80	350	200	200	200
20	6.20	3.65	2.90	400	200	200	200
5	7.40	4.30	3.10	400	400	400	400
	8.05	4.70	3.30	999999	999999	999999	999999

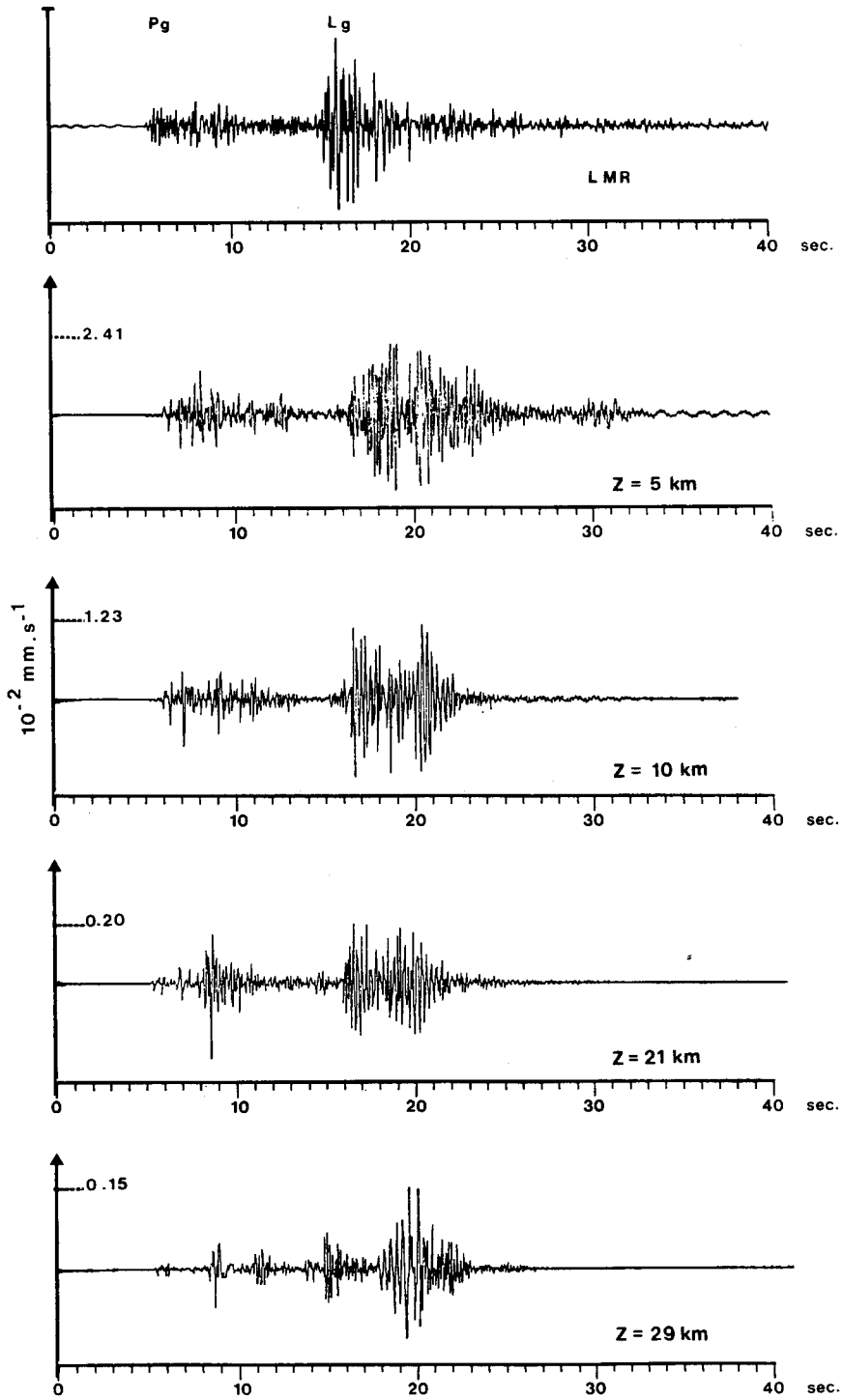

Fig. 6. Synthetic seismograms (vertical velocity component) obtained for event 2 at an epicentral distance of 162 km by using the crustal model of Table 3(a) and different source depths. The amplitude of the maximum of each signal is given in hundredths of a millimeter. These seismograms are compared with the observed record at station LMR.

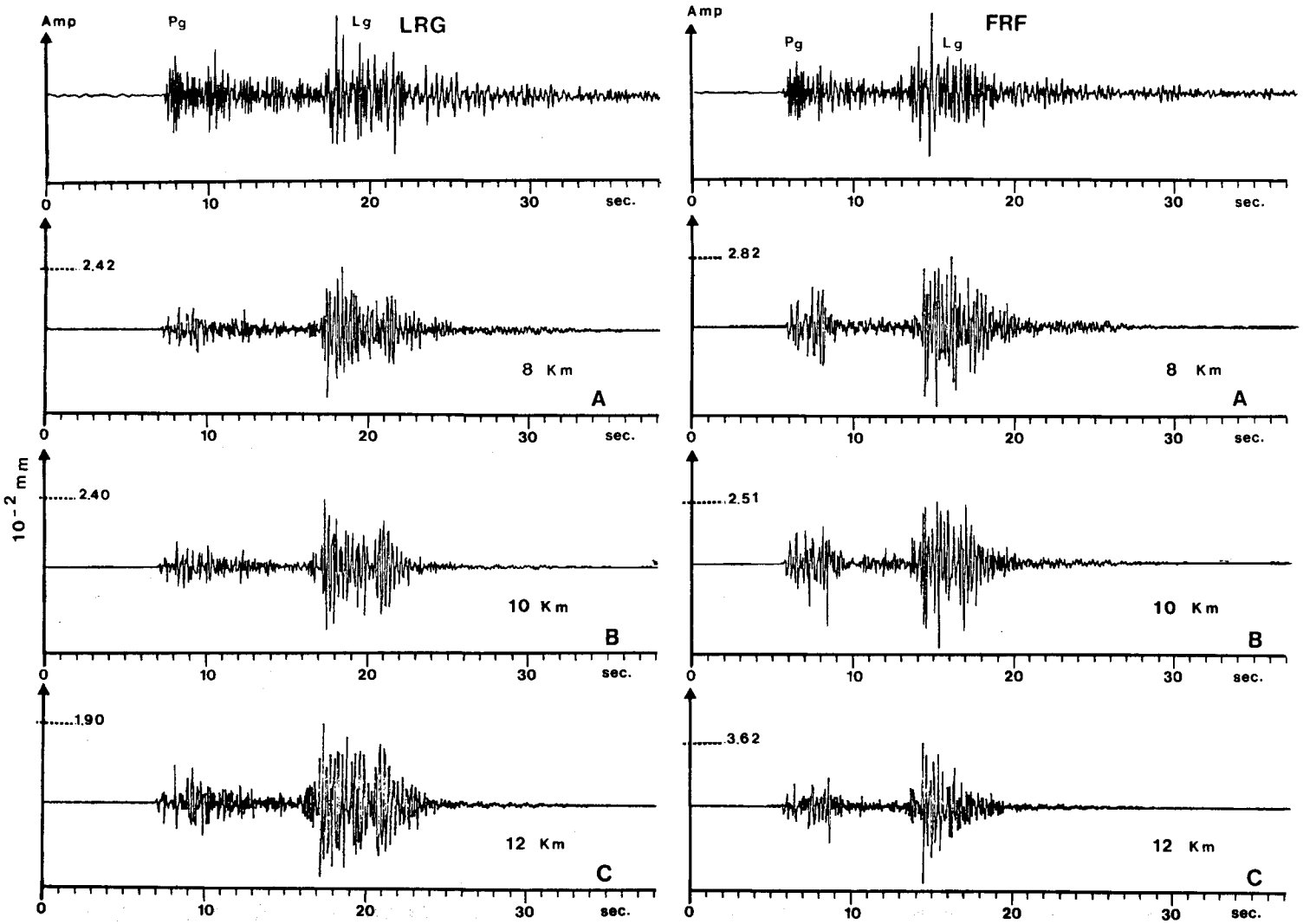

Fig. 7. Synthetics corresponding to the fitting of the source depth for event 2. These seismograms are calculated for an epicentral distance of 134 km (station FRF) and 156 km (station LRG). The crustal model is the same as in the previous figure. Quality factors used are depicted in Table 3(b) with $Q_p = 2Q_s$.

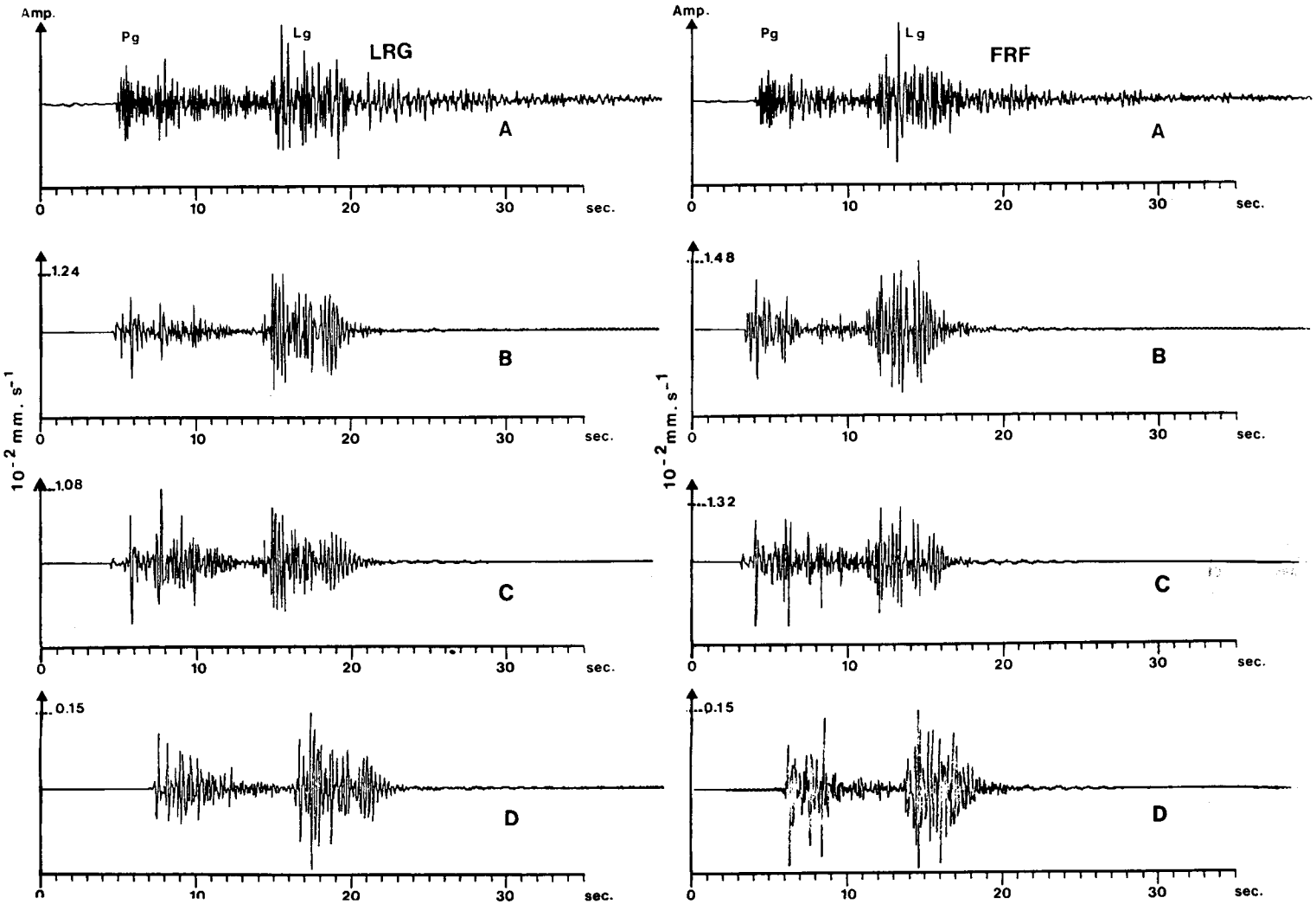

Fig. 8. Comparison between the observed records at stations FRF and LRG from event 2 (A) and the synthetics computed with different crustal models, for a focal depth of 10 km. B. The crustal model as depicted in Table 3. C. The crustal model as depicted in Table 2. D. The Moho depth is chosen as 40 km. The Q values are reported in Table 3 (c) with $Q_p = Q_s$.

km deep, as was found southwest of the epicenter (Fig. 1), this model corresponds to the actual structure on a rather important part of the ray path, but the synthetics computed for stations LRG and FRF are clearly different from the observed seismograms (Fig. 8D).

Other focal depth values have been tested in computations using the two crustal models described above. None of these trials provided fits as realistic as those obtained previously.

The conclusion of these tests is that the best crustal model for the simulation seems to be the most characteristic of the structure of the crust just around the epicenter.

4. An earthquake beneath the Ligurian Sea

This event occurred on October 4, 1985, at 15 h 22. It was located at 43.6°N ± 0.02°, 8.0°E ± 0.02, $z = 10$ km as computed by E.M.S.C. The location from L.D.G. is given with a focal depth of 14 km whereas according to I.G.G. the depth is 18 km. The focal mechanism indicates reverse faulting (Table 1). The crustal structure in the Ligurian sea is known from numerous seismic sounding surveys [1,2]. The starting crustal model deduced from these studies is reported in Table 4. At first the quality factors are assumed to be constant with depth: $Q_s = 200$, $Q_p = 400$ (Table 4,a).

4.1. Effect of depth

The wave trains observed at station CVF (Fig. 9) are characterized by an emergent shape typical of the propagation in the oceanic crust. Another feature of oceanic propagation is the absence of P_g and L_g waves [21]. This seismogram is very different from the ones analyzed in the previous examples. In order to check the sensitivity to focal depth, we computed synthetic seismograms for a point dislocation at depths 6 km, 9 km, 12 km, and 18 km. The synthetics corresponding to station CVF are depicted in Fig. 9.

In the case of the two shallower sources (6 and 9 km) the synthetics exhibit characteristics completely different from those of the observed seismograms. The waves guided in the sedimentary layers give rise to very long and energetic coda (see Fig. 9B where the depth is 6 km). When the focus is in the volcanic layer ($z = 9$ km), we still obtain a strong excitation of guided waves (Fig. 9C). If the source is located in the lower crust (layer "3b"), the fit between actual and theoretical seismograms is better (Fig. 9D). When the focus is in the mantle the P waves are more impulsive (Fig. 9E).

The fit with observed seismogram, P-wave arrival-times and global shape of the wave train, leads to choose a source in the lower crust which is only 4 km thick (Table 4,a), that is to say an intermediate depth between 10 and 14 km. A depth of 12 km is used in the following computations.

4.2. Discussion

The first synthetics displayed in Fig. 9 are computed with average quality factors $Q_s = 200$ and $Q_p = 2Q_s$. Then, values increasing with depth are used (Table 4,b) with low values for Q in the sedimentary and volcanic layers. The seismogram synthesized by using these values is depicted in Fig. 10B and may be compared with the one

TABLE 4

Crustal model and different quality factors used for event 3. $Q_p = 2Q_s$ in cases (a) and (b)

Layer thickness (km)	P-wave velocity (km/s)	S-wave velocity (km/s)	Density (g/cm^3)	(a) Q_s	(b) Q_s	(c) Q_p	(d) Q_s
2	1.05	0	1.03				
1	1.80	1.06	1.50	200	60	30	60
5	4.40	2.60	2.60	200	80	40	80
2	5.80	3.40	2.70	200	200	100	200
4	6.90	4.10	3.10	200	400	200	400
4 *	7.40 *	4.30 *	3.20 *			200 *	400 *
	8.00	4.70	3.30	999999	999999	999999	999999

* Used for stations LRG and FRF (case c) in order to simulate the behavior of the wave train crossing the continental slope.

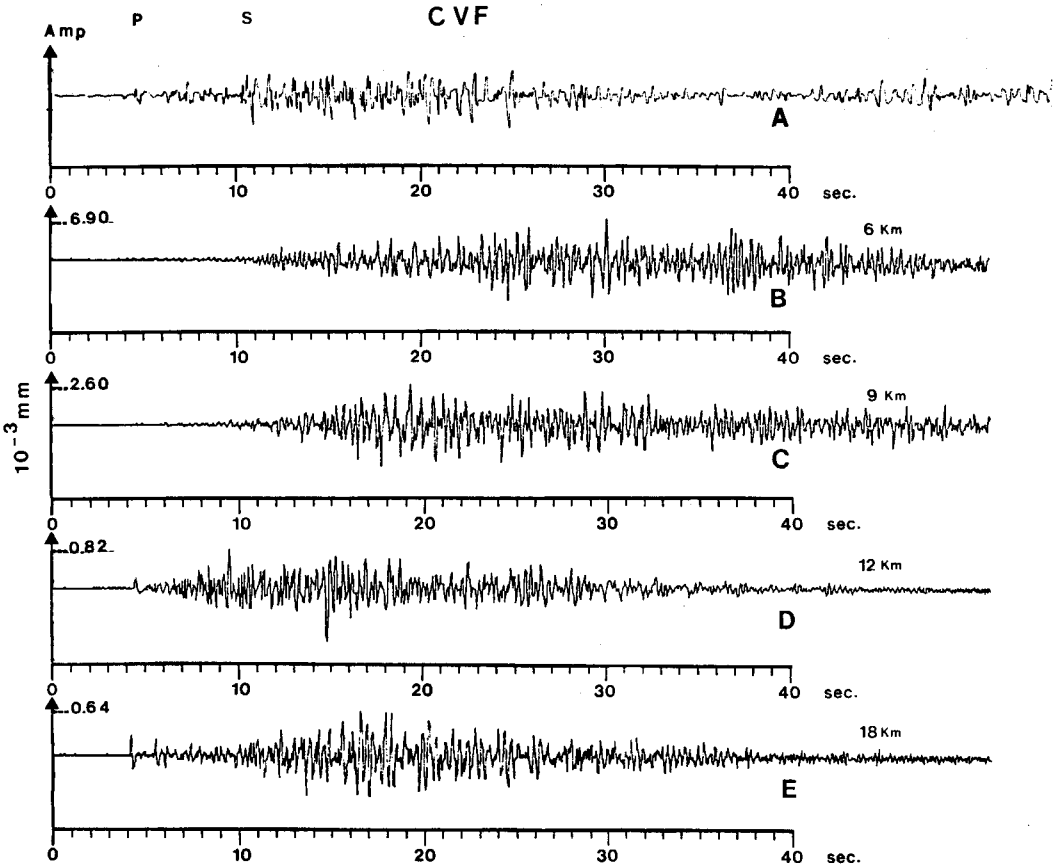

Fig. 9. Comparison between the observed record (vertical displacement component) at station CVF from event 3 (A) and the synthetic seismograms computed with the source located in different layers. B. The focus is in the Messinian sedimentary layer (6 km). C. The focus is in the volcanic layer (9 km). D. The focus is in the lower crust (12 km). E. The focus is in the mantle (18 km). The crustal model and quality factors used are reported in Table 4(a). The maximum of amplitudes are given in microns.

computed with constant quality factors (Fig. 10C). The ratio between P and S amplitudes is now more realistic.

The importance of the water layer present in our crustal model along the entire ray-path is illustrated by computing a synthetic seismogram with the same crustal model but where the water layer is replaced by a thicker sedimentary layer. The result is shown in Fig. 10D. The comparison with the Fig. 10C indicates that the water column does not play an important part on the seismogram shape but produces a global decrease of the energy.

The synthetic signals corresponding to stations LRG and FRF are characterized by a lack of energy pulses in comparison with the actual wave trains, as shown in Fig. 11B, where the quality factors depicted in Table 4(b) are used. Examining the different ray-paths (Fig. 1), one can observe that the seismic waves towards the Corsican station CVF cross the oceanic crust and undergo a sharp transition between the oceanic and continental crust in the vicinity of the station. Towards the stations FRF and LRG the ray-paths mainly cross the continental slope which is an intermediate domain between the oceanic and continental crust and where the Moho is dipping from 14 up to 35 km under the stations [1]. In order to take into account this slope of the Moho, we introduce in the model a fictitious transition layer beneath the oceanic crust, as displayed in Table 4(c). Fig. 11A and C show the comparison between the computed and observed wave-trains. We may notice that this crustal model enhances P-wave arrivals. To obtain a better fit, the quality factors have been checked. Very low values of Q_p

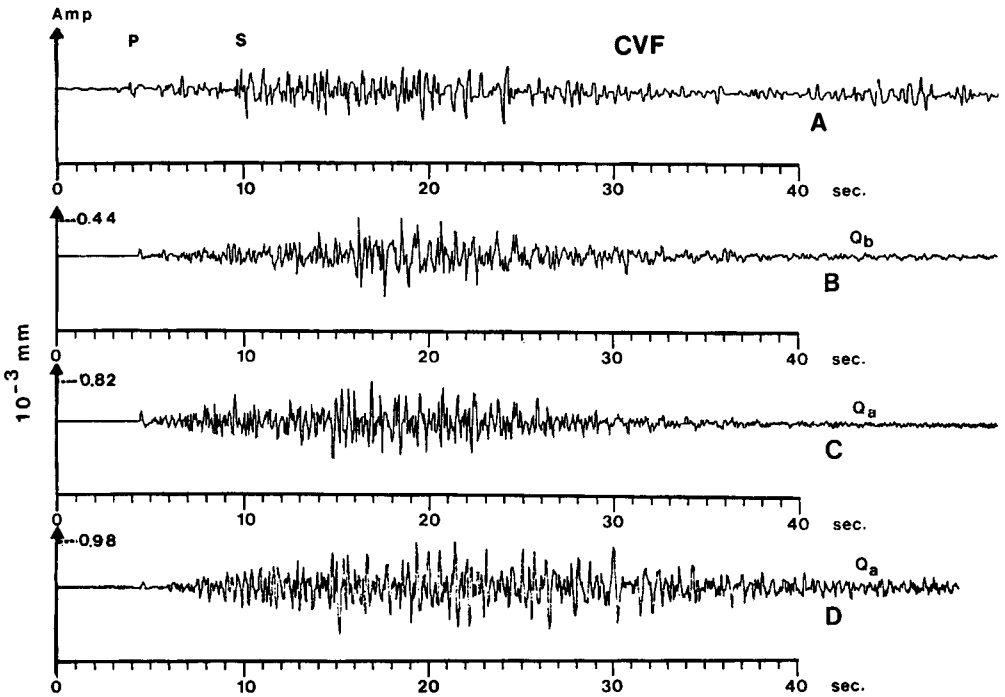

Fig. 10. Comparison between the observed record at station CVF from event 3 (A), epicentral distance 134 km, and the synthetics computed with different quality factors depicted in Table 4 (a: signal C; b, signal B). For the seismogram reported in D the water layer is replaced by a sedimentary layer with a P-wave velocity of 1.8 km. The focus depth is 12 km for each computation.

are necessary to get a realistic aspect in the synthetics (Table 4,c). Once again, this apparent attenuation of P waves should be linked to strong lateral changes along the path between the source and the stations.

5. Conclusion

The discrete wave number method was used to model seismograms at distances from 80 to 160 km.

As a first step, this method was applied to a rather homogeneous area (first example) and a reliable crustal model introduced in the computations allows the recorded wave trains to be described with a good accuracy. For the two other examples the wave trains crossed heterogeneous media. In the second example, the most realistic synthetics were obtained with a crustal model characteristic of the structure of the area around the epicenter: the region of Ivrea. For the third example, an earthquake in the oceanic domain, good results were obtained when the ray-path, from the source to the station is mainly oceanic. For the other stations, the ray path mainly crosses the continental margin; the introduction of a fictituous intermediate layer at the bottom of the crust allows to obtain realistic synthetics.

We noticed that the envelopes of the seismograms are very dependent on the focal depth. Therefore, if a convenient crustal model and a precise focal mechanism are used in the computation, we may constrain the depth of the source in a better way than with the standard location methods that use arrival times, as we showed in the first example. If the structure changes from the source area to the receiver, we deduced from our modelings, that the crustal model providing the most realistic synthetics is this one describing the structure in the vicinity of the epicenter. In this last case, we may assume that the depth, deduced from the computation, may be realistic, although not so accurate as the determination obtained in the first example.

The waveforms show a much weaker sensitivity to slight variations of the crustal structure than to the source depth. Nevertheless, we have seen that the computation of realistic synthetics involves

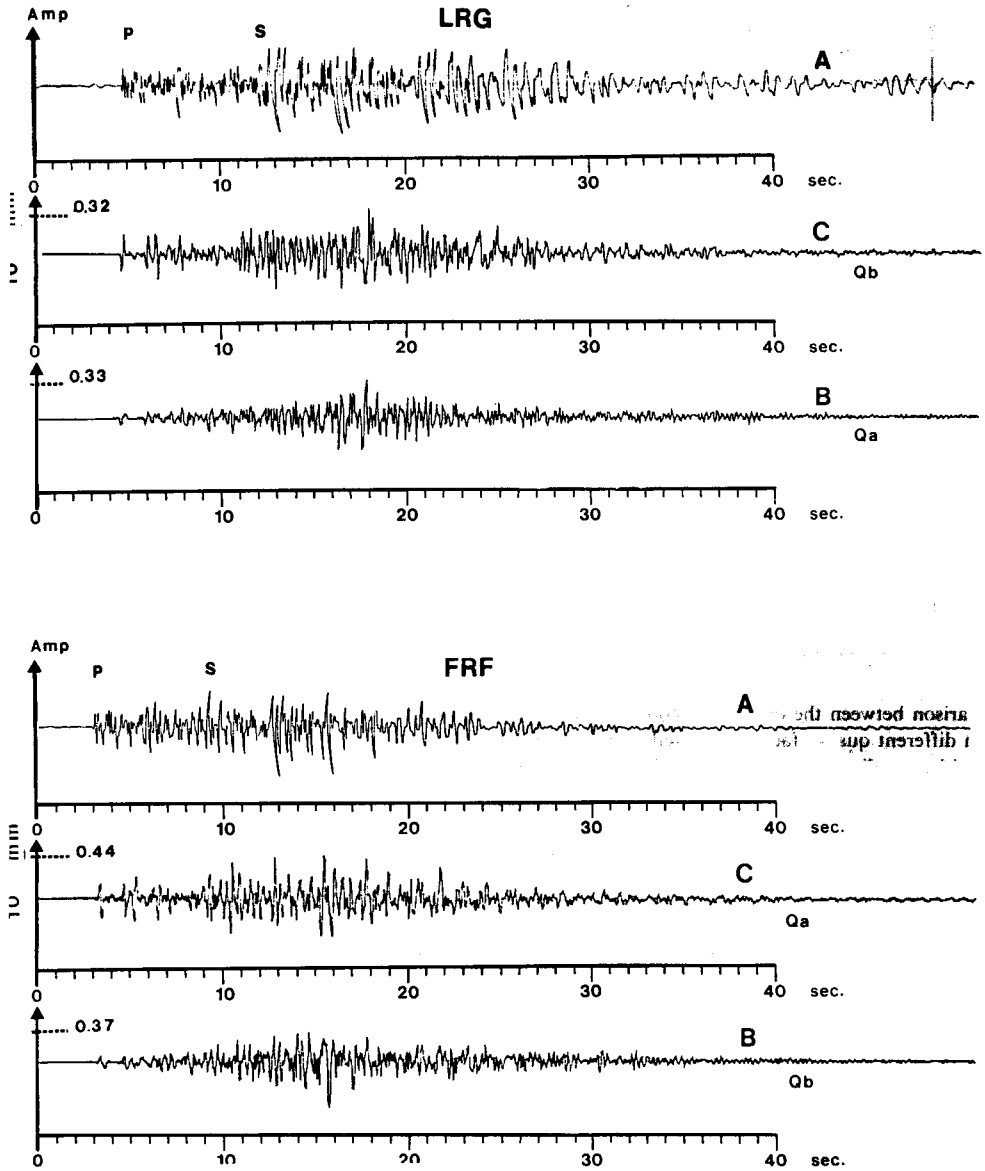

Fig. 11. Comparison between the observed records (vertical displacement component) at stations LRG and FRF from event 3 (A), corresponding to epicentral distances of 116 km and 132 km and synthetic seismograms computed: (B) with the crustal parameters shown in Table 4 (a); (C) in adding a transitional layer as shown in Table 4(c).

few degrees of freedom for the crustal model which, therefore may be improved by the fitting of the synthetics.

By modeling seismograms from an hetereogeneous region we have pointed out the importance of apparent anelastic attenuation. The good fit of the ratios of P to S amplitudes obtained between synthetics and observed seismograms lead us to introduce quality factors that increase with depth. The more the ray-paths cross an heterogeneous medium, the weaker is the apparent ratio Q_p/Q_s as already explained by Richards and Menke [22].

We studied three earthquakes with well constrained focal solutions. However, in order to study the sensitivity of the waveform to the source mechanism, we computed synthetics with small variations of the focal parameters. The azimuth or dip of the fault planes were changed by about 20°

(these perturbed mechanisms are displayed in Table 1). This variation corresponds to the accuracy usually accepted for a focal solution computed with regional networks. The numerical results suggest that the L_g waveforms are weakly sensitive to small changes in the focal solutions, while the amplitude of first P-wave arrival was sometimes clearly modified. Nevertheless, in the examples studied, the overall characteristics of the envelopes of the signals are not significantly disturbed by slight variations in the direction of the nodal planes. Therefore, the uncertainties of focal solutions do not prevent the source depths from being evaluated by modeling with some precision.

We have focused our work on the source depth determination by visual analysis of the waveforms. Depth is deduced from the overall similarity between observed and synthetic wave trains, that is to say by qualitative criteria. These first results suggest to use more quantitative approach, even if it is not possible to simply retrieve the depth by inversion owing to the non-linearity of the problem in a multi-layered medium and the large number of unknown parameters. The ratio between P_g and L_g amplitude is strongly linked to the source location because the P_g wave exitation is mostly insensitive to the focal depth while the energy of L_g waves decreases notably with a deeper source. Nevertheless we have pointed out the influence of apparent attenuation in the observed ratio of P to S amplitudes. Thus, the simple calculation of this parameter is not sufficient to evaluate the depth, but may be a rough indicator. In the above discussions, we have chosen the values of depth by looking at the variations of the shape of the wave trains, mainly L_g waveform, the duration of the coda and the temporal coherence between the different energy pulses. In fact, the method is obviously founded on the optimization of similarity of the signal envelopes. The computation of the cross-correlation between observed and synthetic envelopes should be a good quantitative approach to constrain the source depth.

Acknowledgements

We are grateful to D. Hatzfeld and the two anonymous reviewers who provided enlightening comments to improve the manuscript. We thank P.Y. Delpech for his assistance.

References

1 J.P. Rehault, Evolution tectonique et sédimentaire du Bassin Ligure (Méditerranée occidentale), 128 pp., Thèse d'Etat VI Paris, 1981.
2 S. Le Douaran, J. Burrus and F. Avedik, Deep structure of the North-Western Mediterranean basin: results of two-ship seismic surveys, 1984.
3 M. Bouchon, The complete synthesis of seismic crustal phases at regional distances, J. Geophys. Res. 87, 1735–1741, 1982.
4 R.B. Hermann and A. Kijko, Modeling some empirical L_g relations, Bull. Seismol. Soc. Am. 73, 157–172.
5 W.Y. Kim, Modeling short-period crustal planes at regional distances for the seismic source parameters inversion, Phys. Earth Planet. Inter. 57, 159–178, 1987.
6 M. Campillo, J.L. Planchet and M. Bouchon, Frequency dependent attenuation in the crust beneath central France from L_g waves: data analysis and numerical modeling, Bull. Seismol. Soc. Am. 75, 1395–1411, 1985.
7 M. Bouchon and K. Aki, Discrete wave-number representation of seismic source wave fields, Bull. Seismol. Soc. Am. 67, 259–277, 1977.
8 M. Bouchon, A simple method to calculate Green's function for elastic layered media, Bull. Seismol. Soc. Am. 71, 959–971, 1981.
9 M. Campillo, M. Bouchon and B. Massinon, Theoretical study of the excitation, spectral characteristics and geometrical attenuation of regional seismic phases, Bull. Seismol. Soc. Am. 74, 79–90, 1984.
10 N. Bethoux, M. Cattaneo, P.Y. Delpech, C. Eva and J.P. Rehault, Mécanismes au foyer de séismes en mer Ligure et dans le sud des Alpes occidentales: résultats et interprétation, C.R. Acad. Sci., Paris, Sér. 2, 307, 71–77, 1988.
11 K. Aki, Quantitative Seismology Theory and Methods. Freema, 1980.
12 M. Nicolas, B. Massinon, P. Mechler and M. Bouchon, Attenuation of regional phases in Western Europe, Bull. Seismol. Soc. Am. 72, 2089–2106.
13 M. Recq, Structure de la croûte terrestre en Provence, d'après les expériences du Revest et du Lac Nègre, C.R. Acad. Sci. Paris, Sér. D 264, 1588–1591, 1967.
14 D.L. Anderson and C.B. Archambeau, The anelasticity of the earth, J. Geophys. Res. 69, 2071–2084, 1964.
15 R.M. Clowes and E.R. Kanasewich, Seismic attenuation and the nature of reflecting horizons within the crust, J. Geophys. Res., 75, 6693–6705, 1970.
16 F. Thouvenot, Frequency dependence of the quality factor in the upper crust: a deep seismic sounding approach, Geophys. J.R. Astron. Soc. 73, 427–447, 1983.
17 P.J. Carpenter and A.R. Sanford, Apparent Q for upper crustal rocks of the central Rio Grande Rift, J. Geophys. Res. 90, 8661–8674, 1985.
18 M.N. Toksoz, A.H. Dainty, E. Reiter and R.S. Wu, A model for attenuation and scattering in the earth's crust, Pure Appl. Geophys. 128, 81–100, 1988.
19 J. Ansorge, St. Mueller, E. Kissling, I. Guerra, C. Morelli and S. Scarascia, Crustal section across the zone of Ivrea-Verbano from the Valais to the Lago Maggiore, Boll. Geof. Teor. Appl. 21, 83, 149–157, 1979.

20 R. Bayer, M. Cazes, G.V. Dal Piaz, B. Damotte, G. Elter, G. Gosso, A. Hirn, R. Lanza, B. Lombardo, J.L. Mugnier, A. Nicolas, R. Nicolich, R. Polino, F. Roure, R. Sacchi, S. Scarascia, I. Tabacco, P. Tapponnier, M. Tardy, M. Taylor, F. Thouvenot, G. Torreilles and A. Villien, Premiers résultats de la traversée des Alpes occidentales par sismique réflexion verticale (programme ECORS-CROP), C.R. Acad. Sci. Paris, Sér. 2, 305, 1461–1470, 1987.

21 M. Ewing, W.S. Jardetsky and F. Press, Elastic Waves in Layered Media, McGraw-Hill, New York, N.Y., 1957.

22 P.G. Richards and W. Menke, The apparent attenuation of a scattering medium, Bull. Seismol. Soc. Am. 73(4), 1005–1021, 1983.

23 A. Hirn, Le cadre structural profond d'après les profils sismiques, in: Evolutions géologiques de la France, A. Autran and J. Dercourt, eds., 26ème Congr. Géol. Int. Colloq. C7, Mém. B.R.G.M., Fr. 107, 34–39, 1980.

24 R. Meissner, The Continental Crust, A Geophysical Approach, 426 pp., Academic Press, London, 1986.

25 C. Morelli, P. Giese, M.T. Carrozzo, B. Colombi, A. Hirn, H. Letz, R. Nicolich, C. Prodehl, C. Reichert, P. Rower, M. Sapin, S. Scarascia and P. Wigger, Crustal and upper mantle structure of the Northern Apennines, the Ligurian Sea and Corsica, derived from seismic and gravity data, Boll. Geofis. Teor. Appl. 19, 199–260, 1977.

26 J.P. Rehault, G. Boillot and A. Mauffret, The Western Mediterranean Basin geological evolution, Mar. Geol. 55, 447–477, 1984.

27 H. Closs and Y. Labrouste, Recherches sismologiques dans les Alpes occidentales au moyen des grandes explosions en 1956, 1958 et 1960, C.N.R.S., 1963.